Synthetic Metals 268 (2020) 116504

Contents lists available at ScienceDirect

Synthetic Metals

journal homepage: www.elsevier.com/locate/synmet

Yellowish-orange and red emitting quinoline-based iridium(III) complexes: Synthesis, thermal, optical and electrochemical properties and OLED application

Nuray Altinolcek[a], Ahmet Battal[b,c], Mustafa Tavasli[a,*], Joseph Cameron[c], William J. Peveler[c], Holly A. Yu[c], Peter J. Skabara[c]

[a] Uludag University, Faculty of Science-Art, Department of Chemistry, 16059, Nilufer, Bursa, Turkey
[b] Mus Alparslan University, Faculty of Education, 49100, Mus, Turkey
[c] WestCHEM, School of Chemistry, University of Glasgow, Joseph Black Building, G12 8QQ, Glasgow, UK

ARTICLE INFO

Keywords:
Formyl group
2-Phenylquinoline
Iridium
Heteroleptic
Phosphorescence
Electroluminescence

ABSTRACT

Two novel heteroleptic iridium(III) acetylacetonate (acac) complexes **K3a** and **K3b** were synthesised from cyclometallating ligands of 2-(4′-formylphenyl)quinoline **11a** and 2-(5′-formylphenyl)quinoline **11b**. Complexes **K3a** and **K3b** were fully characterised by NMR spectroscopy, mass spectrometry and FT-IR. Differential scanning calorimetry (DSC) and thermal gravimetric analysis (TGA) indicate that both complexes were amorphous solids, stable up to 303 °C and 313 °C, respectively. Complexes **K3a** and **K3b** showed strong, high-energy absorption bands (< 400 nm) due to ligand-centred (^{1}LC) transitions and weaker, low-energy absorption bands (400 − 600 nm) arising from a mixture of metal-to-ligand charge transfer (^{1}MLCT/^{3}MLCT) and ligand-centred (^{3}LC) transitions. In degassed dichloromethane solutions, complexes **K3a** and **K3b** gave yellowish-orange and red phosphorescent emissions at 579 nm and 630 nm, with quantum efficiencies of 99.3 % and 79.3 %, respectively. At positive potential, complexes **K3a** and **K3b** exhibited a one-electron reversible oxidation ($E^{ox}_{1/2}$) peak at 0.69 V and a quasi-reversible oxidation ($E^{ox}_{1/2}$) peak at 0.60 V, respectively, which were assigned to the Ir(III)/Ir(IV) couple. At negative potentials, complexes **K3a** and **K3b** exhibited a one-electron irreversible reduction peak at -1.79 V and -1.94 V, respectively. Phosphorescent organic light-emitting diodes (PhOLEDs) were fabricated with a device configuration of ITO/PEDOT:PSS/EML/TPBi/LiF/Al, in which **K3a** and **K3b** gave yellowish-orange and red electroluminescence (EL) at 572 nm and 628 nm, respectively. Complex **K3a** gave the highest luminance of 2773 cd/m^2, current efficiency of 3.3 cd/A, external quantum efficiency of 1.2 % and maximum power efficiency of 1.05 lm/W with a turn-on voltage of 5.0 V (Device A).

1. Introduction

Iridium(III) complexes have found many different applications in the area of sensors, OLEDs, medicine, bioimaging etc [1,2]. Iridium(III) complexes have excellent chemical and thermal stabilities, high phosphorescence quantum yields and relatively short phosphorescence lifetimes [3–9]. Additionally, facile colour tuning is also possible through modifications of ligand structure [9–11]. In this regard, different cyclometallating ligands have been synthesised with the electron-withdrawing/donating groups attached to different positions of the ligand to configure the colour of many iridium(III) complexes [12–14].

In general, iridium(III) complexes have been synthesised in two different forms - homoleptic or heteroleptic [15,16]. The former type of complexes have three identical cyclometallating ligands, whereas the latter complexes have two identical cyclometallating ligands and an ancillary ligand [16,17]. Heteroleptic iridium(III) complexes can be synthesised in high yields as compared to homoleptic iridium(III) complexes.

In OLED devices, iridium(III) complexes are frequently used as dopant materials in the emissive layer [18,19]. Iridium(III) complexes that emit light in three basic colours (blue, green and red) are available in the literature as benchmark materials [20]. Bis(2-(1′-benzothien-2′-yl) pyridinato-*N*,C3′)iridium(acetylacetonate) ($Ir(btp)_2acac$) [21,22] and tris(1-phenylisoquinoline)iridium(III) ($Ir(piq)_3$) [23] are considered as red-emitting benchmark materials. A number of red-emitting iridium

* Corresponding author.
E-mail address: mtavasli@uludag.edu.tr (M. Tavasli).

https://doi.org/10.1016/j.synthmet.2020.116504
Received 19 May 2020; Received in revised form 18 June 2020; Accepted 6 July 2020
Available online 11 July 2020

(III) complexes have been designed and synthesised in the literature [24–26]. Recently they have been used in fabricating white OLEDs and in the near future they may find application in traffic signals and automobile brake lights [27]. However, the low luminescent quantum yields of these complexes make them unsuitable for practical usage [28,29]. Therefore there is continuing interest in designing and synthesising highly red emissive iridium(III) complexes [30].

High electron affinities were observed for quinoline-based cyclometallating ligands [31] such as 2-phenylquinoline (pq) and 1-phenylisoquinoline (piq). From these ligands two parent heteroleptic iridium (III) acetylacetonate (acac) complexes, $Ir(pq)_2acac$ and $Ir(piq)_2acac$, were prepared. The former complex gave orange electroluminescence (EL) and the latter complex gave red EL [6,32,33]. To tune emission colour and to improve material properties and device performances, many different electron withdrawing and donating groups have been grafted on to the *ortho-/meta-/para*-positions of C-ring and/or N-ring of pq and piq cyclometallating ligands [31,34–40]. In this work, Ir $(pq)_2acac$ was chosen as parent complex, the formyl group was chosen as an electron withdrawing and conjugation enhancing group, and the *meta*- and *para*-positions of the C-ring were chosen as grafting positions. Very recently it was shown by us [41] that the formyl group is a simple and good acceptor for D-A systems, and others [42,43] also chose it to explore its tuning properties in OLEDs. Depending on which position of the C-ring the formyl group is grafted, the highest occupied molecular orbital (HOMO) energy levels could be altered. Thus, the emission of the parent complex could be fine-tuned, and the material properties and device performances could be improved. To demonstrate this, 2-(4′/5′-formylphenyl)quinolines **11a** and **11b** were prepared as cyclometallating ligands. These ligands were then converted into two novel heteroleptic iridium(III) complexes **K3a** and **K3b**, where a formyl group was positioned at the *para*-position and *meta*-position to iridium. Here we report the synthesis, thermal, optical, electrochemical and electroluminescent properties of these complexes **K3a** and **K3b**.

2. Experimental

All reagents were standard reagent grade and purchased from Sigma-Aldrich, Merck and Alfa Aesar. Inert reactions were performed under an argon atmosphere. Nuclear magnetic resonance (NMR) spectra were obtained on an Agilent Premium Compact NMR spectrometer (600 MHz for ^{1}H NMR, 150 MHz for ^{13}C NMR) with tetramethylsilane as internal standard. Elemental analysis was performed on a Costech Elemental system. The IR spectra were obtained (4000–400 cm^{-1}) using a Shimadzu IRAffinity-1S Fourier transform infrared spectrophotometer. The mass spectra were obtained by Bruker microTOFq Mass Spectrometers to obtain low and high resolution spectra using Electron Ionisation (EI) or Electrospray Ionisation (ESI) techniques. UV, PL and photoluminescence quantum yields were measured on a Horiba Duetta two-in-one Fluorescence and Absorbance Spectrometer. Both absorption and emission solutions for reference and samples had a concentration of 10^{-6} M. Cyclic voltammetry (CV) measurements were obtained using a CH Instruments 602E electrochemical workstation with iR compensation using dry dichloromethane. Thermogravimetric analysis was conducted using a Netzsch TG 209 F3 Tarsus Thermogravimetric Analyser under a constant flow of nitrogen. Differential scanning calorimetry was determined on a Netzsch DSC 214 Polyma instrument under a constant flow of nitrogen.

Ligands 11a and **11b.** For the synthesis of **11a** and **11b,** methods of Qian et al. [44] were adapted as follows: 2-bromoquinoline **9**, 3/4-formylphenylboronic acid **10a**/**10b** and potassium carbonate (1 M) were dissolved in THF. The mixture was degassed for 10 min and then dichlorobis-(triphenylphosphine)palladium(II) was added. The reaction mixture was refluxed for 24 h under argon atmosphere. After removing the solvent, the crude product was dissolved in dichloromethane and washed with water (3 × 20 mL). The organic layer was dried over sodium sulfate and then filtered. Upon concentration under reduced pressure and purification by chromatography the title compounds **11a** and **11b** were obtained.

11a: [45,46] A mixture of 2-bromoquinoline **9** (463 mg, 2.2 mmol), 3-formylphenylboronic acid **10a** (500 mg, 3.4 mmol), potassium carbonate (1 M, 27 mL) and dichlorobis(triphenylphosphine)-palladium(II) (33 mg, 0.046 mmol) in THF (15 mL) were reacted as described above, and the crude product purified by flash column chromatography (ethyl acetate:hexane, 1:7 v/v) to give **11a** (414 mg, 80 %) as a white solid. **^{1}H NMR (600 MHz, $CDCl_3$)** δ (ppm): 10.17 (s, 1 H), 8.69 (s, 1 H), 8.49 (d, J = 7.8 Hz, 2 H), 8.28 (d, J = 8.6 Hz, 1 H), 8.19 (d, J = 8.4 Hz, 1 H), 7.99 (d, J = 7.6 Hz, 1 H), 7.94 (d, J = 8.6 Hz, 1 H), 7.86 (d, J = 8.1 Hz, 1 H), 7.76 (t, J = 7.7 Hz, 1 H), 7.70 (t, J = 7.6 Hz, 1 H), 7.57 (t, J = 7.6 Hz, 1 H). **FT-IR ($\bar{\upsilon}$ cm^{-1}):** 2875, 2866, 2852, 2829, 2809, 2757, 1689.

11b: [47] A mixture of 2-bromoquinoline **9** (231 mg, 1.1 mmol), 4-formylphenylboronic acid **10b** (250 mg, 1.7 mmol), potassium carbonate (1 M, 14 mL) and dichlorobis-(triphenylphosphine)palladium(II) (16 mg, 0.023 mmol) in THF (10 mL) were reacted as descirbed above and purified by preparative thin layer chromatography (ethyl acetate:dichloromethane, 1:18 v/v), to give **11b** (226 mg, 87 %) as a white solid. **^{1}H NMR (600 MHz, $CDCl_3$)** δ (ppm): 10.11 (s, 1 H), 8.35 (d, J = 8.2 Hz, 2 H), 8.27 (d, J = 8.6 Hz, 1 H), 8.18 (d, J = 8.5 Hz, 1 H), 8.04 (d, J = 8.1 Hz, 2 H), 7.92 (d, J = 8.5 Hz, 1 H), 7.86 (d, J = 8.1 Hz, 1 H), 7.77 (dd, J = 8.4, 1.4 Hz, 1 H), 7.57 (d, J = 7.3 Hz, 1 H). **FT-IR ($\bar{\upsilon}$ cm^{-1}):** 2925, 2866, 2817, 2790, 2765, 1682.

Diiridium complexes D3a and **D3b.** For the synthesis of **D3a** and **D3b** methods of Sprouse et al. [48] were adapted as follows: iridium trichloride hydrate ($IrCl_3.xH_2O$) and the ligand **11a**/**11b** were mixed in a 3:1 mixture of 2-ethoxyethanol:water (v/v). The mixture was degassed for 10 min and was then heated at 110 °C for 24 h under argon atmosphere. After cooling, the precipitate was filtered off and then washed with ethanol to aff ;ord the title complexes **D3a** and **D3b** as solids. Both diiridium complexes **D3a** and **D3b** were used in the next step without further purifications.

D3a: A mixture of $IrCl_3.xH_2O$ (116 mg, 0.4 mmol) and ligand **11a** (226 mg, 0.97 mmol) in 2-ethoxyethanol:water (12 mL, 3:1 v/v) gave **D3a** (160 mg, % 60) as an orange solid. **^{1}H NMR (600 MHz, $CDCl_3$)** δ (ppm): 9.75 (s, 1 H), 8.49 – 8.32 (m, 1 H), 8.22 – 8.01 (m, 1 H), 8.01 – 7.79 (m, 2 H), 7.56 – 7.43 (m, 1 H), 7.32 (s, 1 H), 6.98 – 6.68 (m, 2 H), 5.95 (s, 1 H).

D3b: A mixture of $IrCl_3.xH_2O$ (227 mg, 0.8 mmol) and ligand **11b** (443 mg, 1.9 mmol) in 2-ethoxyethanol:water (16 mL, 3:1 v/v) gave **D3b** (350 mg, 67 %) as a dark red-brown solid. **^{1}H NMR (600 MHz, d_6-DMSO)** δ (ppm): 9.47 (s, 1 H), 9.42 – 9.34 (m, 1 H), 8.69 (d, J = 8.6 Hz, 1 H), 8.54 (d, J = 8.7 Hz, 1 H), 8.19 (d, J = 8.0 Hz, 1 H), 8.15 – 8.09 (m, 1 H), 7.71 – 7.63 (m, 2 H), 7.36 (d, J = 7.9 Hz, 1 H), 6.65 (s, 1 H).

Heteroleptic iridium(III) complexes K3a and **K3b.** For the synthesis of **K3a** and **K3b** methods of Lamansky et al. [6] were adapted. A mixture of diiridium complex **D3a**/**D3b**, acetyl acetone, sodium carbonate and 2-ethoxyethanol was degassed under argon for 15 min. The reaction mixture was then heated at 100 °C for 15 min and was allowed to cool to room temperature. After cooling, the precipitate was filtered off and then dissolved in dichloromethane. The organic layer was washed with water (3 × 20 mL), dried over sodium sulfate and then filtered. Upon concentration under reduced pressure and purification, the title compounds **K3a** and **K3b** were obtained.

K3a: A mixture of **D3a** (227 mg, 0.16 mmol), acetyl acetone (41 mg, 0.41 mmol) and sodium carbonate (122 mg, 1.15 mmol) in 2-ethoxyethanol (16 mL) were reacted as above. Upon preparative thin layer chromatography (ethyl acetate:dichloromethane, 1:9 v/v) and recrystallisation from a mixture of dichloromethane:acetone (1:1 v/v) **K3a** (100 mg, 41 %) was prepared as orange crystals. **^{1}H NMR (600 MHz, d_6-DMSO)** δ (ppm): 9.89 (s, 1 H), 8.37 (d, J = 8.9 Hz, 1 H), 8.35 – 8.31 (m, 2 H), 8.24 (d, J = 8.7 Hz, 1 H), 7.87 (dd, J = 8.2, 1.6 Hz, 1 H), 7.55 (ddd, J = 8.1, 6.7, 1.2 Hz, 1 H), 7.48 (ddd, J = 8.6, 6.9, 1.6 Hz, 1 H), 7.08 (dd, J = 8.0, 1.7 Hz, 1 H), 6.73 (d, J = 8.0 Hz, 1 H),

4.65 (s, 1 H), 1.51 (s, 3 H). **^{13}C NMR (150 MHz, d_6-DMSO)** δ (ppm): 192.0, 185.8, 168.9, 164.1, 148.8, 148.4, 139.0, 136.7, 131.0, 130.9, 130.0, 128.1, 127.5, 126.7, 126.2,126.1, 116.8, 100.3, 28.1. **FT-IR ($\tilde{u}$ cm^{-1}):** 3055, 2820, 2721, 1676. **MS (ESI, *m/z*):** 779.1480 ([M + Na]$^+$). **HRMS (ESI, *m/z*):** calcd for $C_{37}H_{27}N_2NaO_4Ir$, [M + Na]$^+$, 777.1469, found for [M + Na]$^+$ 777.1435 (Error : +4.3 ppm).

K3b: A mixture of **D3b** (85 mg, 0.13 mmol), acetyl acetone (33 mg, 0.33 mmol) and sodium carbonate (99 mg, 0.94 mmol) in 2-ethoxyethanol (12 mL) were reacted as above. Upon preparative thin layer chromatography (ethyl acetate:dichloromethane, 1:9 v/v) and recrystallisation from a mixture of dichloromethane:acetone (1:1 v/v), **K3b** (40 mg, 20 %) was prepared as dark red-brown crystals. **^{1}H NMR (600 MHz, $CDCl_3$)** δ (ppm): 9.54 (s, 1 H), 8.38 (d, J = 9.0 Hz, 1 H), 8.31 (d, J = 8.7 Hz, 1 H), 8.19 (d, J = 8.6 Hz, 1 H), 7.99 (d, J = 8.1 Hz, 1 H), 7.86 (d, J = 8.0 Hz, 1 H), 7.54 (t, J = 7.4 Hz, 1 H), 7.50 (dt, J = 8.2, 1.5 Hz, 1 H), 7.45 (ddd, J = 8.7, 6.8, 1.6 Hz, 1 H), 6.97 (d, J = 1.7 Hz, 1 H), 4.62 (s, 1 H), 1.48 (s, 3 H). **^{13}C NMR (150 MHz, $CDCl_3$)** δ (ppm): 193.3, 185.7, 169.0, 153.5, 150.2, 149.2, 138.8, 138.4, 135.2, 131.0, 128.0, 127.6, 126.8, 126.4, 126.0, 122.0, 117.3, 100.1, 28.1. **FT-IR ($\tilde{u}$ cm^{-1}):** 3072, 2819, 2711, 1689. **MS (ESI, *m/z*):** 779.1487 ([M + Na]$^+$). **HRMS (ESI, *m/z*):** calcd for $C_{37}H_{27}N_2NaO_4Ir$, [M + Na]$^+$, 777.1469, found for [M + Na]$^+$ 777.1451 (Error : +2.3 ppm)

3. Results and discussion

Synthesis: Complexes **K3a** and **K3b** were synthesised in three steps as depicted in Scheme 1.

The synthesis began with the Suzuki-Miyaura couplings of 2-bromoquinoline **9** and 3-formylphenylboronic acid **10a** or 4-formylphenylboronic acid **10b**, following the methods of Qian et al. [44]. Upon purification by chromatography ligands **11a** and **11b** were obtained in good yields (80 % and 87 %, respectively). Ligands **11a** and **11b** were also reported by others [45–47]. Ligands **11a** and **11b** were then submitted to the cyclometallating reaction with iridium(III) chloride in a mixture of 2-ethoxyethanol and water [48]. These gave chloro-bridged diiridium(III) complexes **D3a** and **D3b** in moderate yields (60–67 %). Diiridium(III) complexes **D3a** and **D3b**, without further purification, were finally submitted to a bridge-splitting reaction with acetylacetone in the presence of sodium carbonate [6]. Upon preparative thin layer chromatography and recrystallisation from a mixture of dichloromethane and acetone, complexes **K3a** and **K3b** were obtained as orange and red-brown crystals, respectively. In comparison to **K3a**, **K3b** was less soluble and less stable in solution. Complexes **K3a** and **K3b** were fully characterised by NMR, FT-IR and MS. Experimental details are given in the Supplementary Material.

Thermal properties: The thermal properties of ligands 11a and 11b and complexes K3a and K3b were investigated by thermogravimetric analyses (TGA). Ligands 11a and 11b were heated to 650 °C and complexes K3a and K3b were heated to 800 °C, with a heating rate of 20 °C/min under nitrogen atmosphere. The decomposition temperatures ($T_d^{5\%}$) corresponding to 5% weight losses for ligands 11a and 11b were 244 °C and 233 °C, respectively, and for complexes K3a and K3b were 303 °C and 313 °C, respectively. TGA curves of all compounds 11a-b and K3a-b are depicted in Fig. 1. These observations suggest that complexes K3a and K3b have similar thermal stabilities to those of other reported iridium(III) acac complexes [37,49] and, if needed, can be vacuum evaporated and, under operating conditions of OLEDs, will not be decomposed readily until 300 °C.

The thermal properties of ligands **11a** and **11b** and complexes **K3a** and **K3b** were also investigated by differential scanning calorimetry (DSC). All compounds **11a-b** and **K3a-b** were first heated to 450 °C and then cooled down to room temperature with a heating rate of 20 °C/min under a nitrogen atmosphere. Both ligands **11a** and **11b** and complexes **K3a** and **K3b** showed only clear melting transitions - ligands **11a** and **11b** at 95 °C and 86 °C, and complexes **K3a** and **K3b** at 314 °C and 321 °C, respectively. Upon first cooling and second heating, no phase transitions for any of the compounds **11a-b** and **K3a-b** were observed. Meanwhile, only complex **K3b** exhibited a glass transition process at 178 °C. In addition, ligands **11a** and **11b** decompose at or above 414 °C and 393 °C, respectively, giving a black charcoal-like residue. This observation suggests that under the operating conditions of OLEDs, with **K3a** no phase segregation should occur in a host-dopant matrix [50]. Fig. 2 shows the DSC curves of compounds **11a-b** and **K3a-b**, and the thermal properties of these compounds are summarised in Table 1.

Electrochemical Properties: Electrochemical redox behaviours (reduction and oxidation) of ligands **11a** and **11b** and complexes **K3a** and **K3b** were investigated by cyclic voltammetry (Fig. 3). Both positive and negative scans were carried out in dichloromethane under argon atmosphere using tetrabutylammonium hexafluorophosphate (0.1 M) as the electrolyte. A conventional three-electrode system was used, with a Pt disk as the working electrode, Ag wire as the reference electrode and Pt wire as the counter electrode. The ferrocene-ferrocenium (Fc/Fc^+) redox couple was used as an internal reference.

At positive potentials, ligands **11a** and **11b** exhibited one-electron irreversible oxidation (E^{ox}_{onset}) peaks at 1.17 V and 1.02 V, respectively. As expected, complexes **K3a** and **K3b** exhibited a single-electron reversible oxidation ($E^{ox}_{1/2}$) peak at 0.69 V and a quasi-reversible oxidation ($E^{ox}_{1/2}$) peak at 0.60 V, respectively. Similar to most cyclometallated iridium(III) complexes [31,37], these lower oxidation potentials were assigned to the Ir^{III}/Ir^{IV} couple. With respect to the oxidation potential of bis(2-phenylquinolyl)-iridium(III)acetylacetonate [$Ir(pq)_2acac$] ($E_{1/2}^{ox}$ = 0.40 V) [32], the formyl group on the phenyl ring increases the oxidation potentials of complexes **K3a** and **K3b**. In addition to that, the formyl group at the *para* position to the iridium (**K3a**) increases the oxidation potential more than that of the *meta* position to the iridium (**K3b**). Similar observations with a fluorine substituent were reported in the work of Zhang et al. [31].

At negative potentials, all compounds exhibited one-electron irreversible reduction (E^{red}_{onset}) peaks at -1.68 V, -1.80 V, -1.79 V and -1.94 V for **11a, 11b, K3a** and **K3b,** respectively.

E_{HOMO} (the highest occupied molecular orbital) and E_{LUMO} (the lowest unoccupied molecular orbital) energy levels of ligands **11a** and **11b** and complexes **K3a** and **K3b** were calculated from the half-wave oxidation/reduction potentials or from the onset of irreversible oxidation/reduction waves. For this the following equations, E_{HOMO} = -(4.8 + $E^{ox}_{1/2}$) and E_{LUMO} = -(4.8 + E_{onset}^{red}) are used [51], in which 4.8 eV was taken as the HOMO energy level of ferrocene (below vacuum level) [52]. The energy gap (E_g) was calculated both from electrochemical data (Eq. 1) and from optical data (Eq. 2).

$$E_g^{elec} = E_{LUMO} - E_{HOMO} \quad (1)$$

$$E_g^{opt} = 1240/\lambda_{onset}^{abs} \quad (2)$$

The optical energy gap (E_g^{opt}) [53–55] was higher than the electrochemical energy gap (E_g^{elec}) for ligands **11a** and **11b,** but was lower for complexes **K3a** and **K3b**. The energy levels are depicted in Fig. 4. The oxidation and reduction potentials and the HOMO-LUMO energy levels of all compounds are summarised in Table 2.

It has been reported for similar Ir(III) complexes that the HOMO lies mainly on the phenyl ring-iridium metal and the LUMO lies mainly on the quinoline ring [27,56]. The formyl group is *para* to the iridium in complex **K3a** and hence its electron withdrawing effect is more pronounced, thus the E_{HOMO} of **K3a** is stabilised compared to **K3b**, where the formyl group is *meta* to iridium. In ligands **11a** and **11b**, the effect of extended conjugation due to the formyl group is more pronounced than the electron withdrawing effect, hence **11b**, where the formyl group is *para* to the quinoline ring, has a smaller energy gap than **11a**, where the formyl group is *meta* to the quinoline ring.

Optical properties: The absorption and photoluminescence (PL) properties of complexes K3a and K3b in dichloromethane were

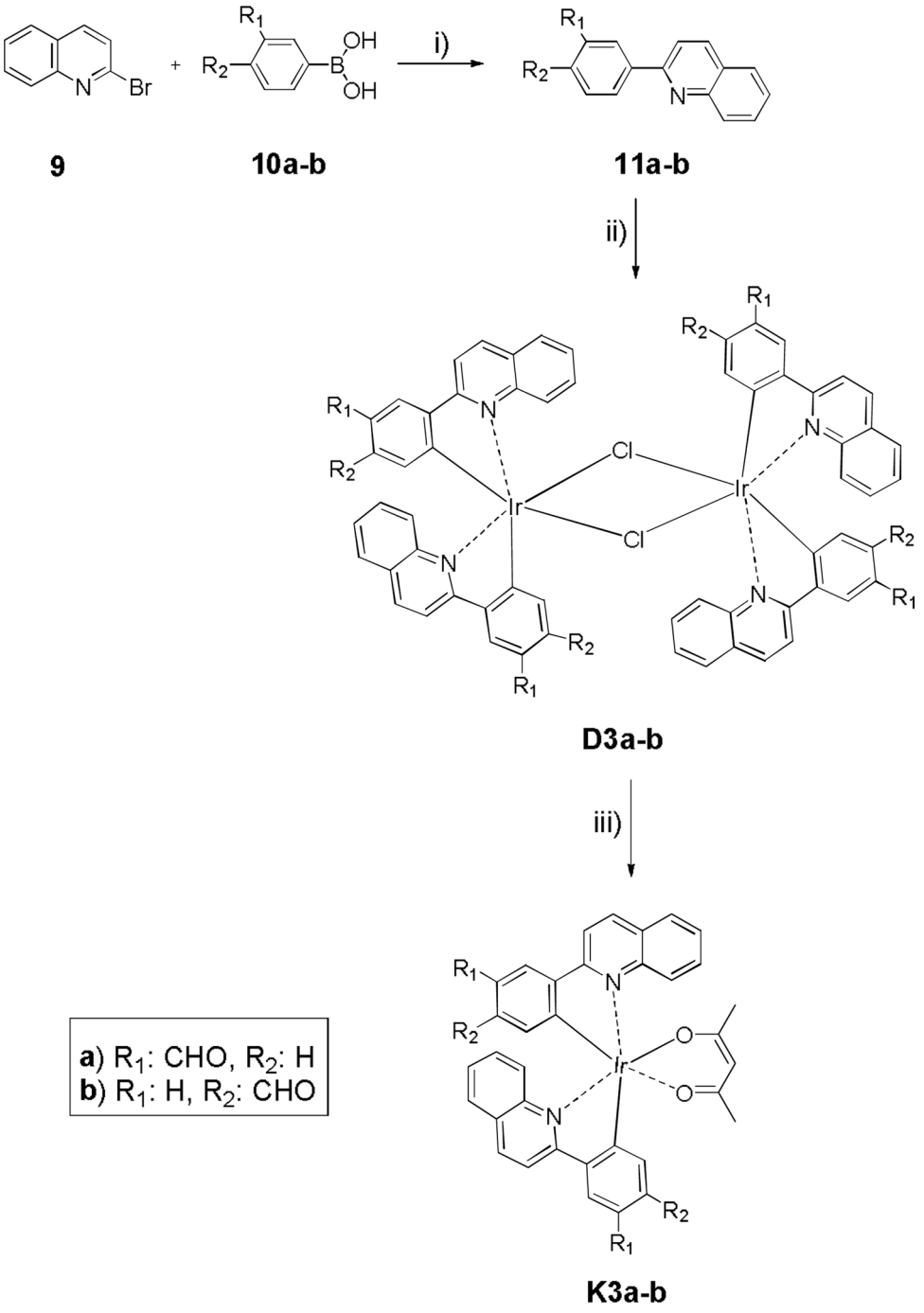

Scheme 1. Synthesis of biscyclometallated iridium(III) acetylacetonate complexes (**K3a** and **K3b**). i) 10a/10b, K_2CO_3, $PdCl_2(PPh_3)_2$, 90 °C, 24 h. ii) $IrCl_3.xH_2O$, 2-ethoxyethanol:water, 110 °C, 24 h. iii) Acetylacetone, Na_2CO_3, 2-ethoxyethanol, 100 °C, 15 min.

investigated by using a Duetta Fluorescence and Absorbance Spectrometer. As seen in Fig. 5, complexes K3a and K3b exhibited two main absorption bands: high-energy strong bands and low-energy, very weak broad bands. The former bands below 400 nm, resembling the absorption of the corresponding free ligands 11a and 11b (see SM, Figure S24) with a slight red shift, were assigned to spin-allowed singlet states of ligand-centred (^{1}LC) and metal-to-ligand charge transfer (^{1}MLCT) transitions. The low-energy, very weak broad bands above 400 nm, missing in the ligands' absorption spectra, were assigned to a mixture of a spin-forbidden triplet state of ligand-centred (^{3}LC) and metal-to-ligand charge transfer (^{3}MLCT) transitions. These assignments were in accordance with previously reported work [31,34,57].

The photoluminescence properties of complexes **K3a** and **K3b** were investigated in degassed dichloromethane solution and the spectra are presented in Fig. 6. Upon excitation at low-energy bands ($\lambda_{exc} > 350$ nm), complexes **K3a** and **K3b** gave yellowish-orange and red phosphorescence emissions at 579 nm and 630 nm, respectively. With respect to $Ir(pq)_2acac$ (λ_{em} = 597 in 2-methyltetrahydrofuran [6] or 599 nm in tetrahydrofuran [32]), the emission of **K3a** was ~20 nm blue-shifted, whereas the emission of **K3b** was ~31 nm red-shifted. The blue shift indicates that the electron withdrawing ability of the formyl group when at the *para* position to the iridium (**K3a**) is more pronounced. The red shift indicates a stronger contribution from the conjugation effect of the formyl group when at the *meta* position to the iridium (**K3b**).

Upon excitation at the highest energy bands ($\lambda_{exc} < 286$ nm),

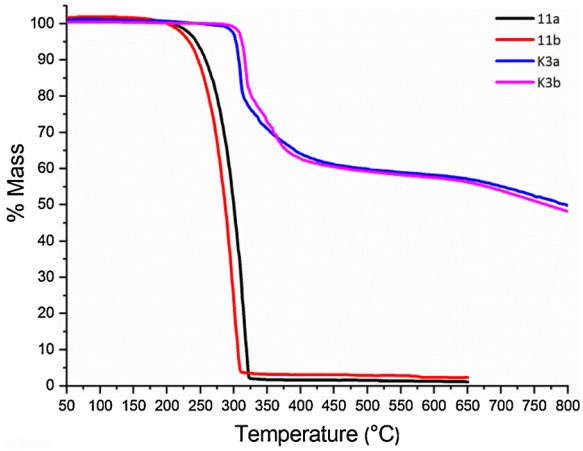

Fig. 1. TGA curves of compounds **11a-b** and **K3a-b.**

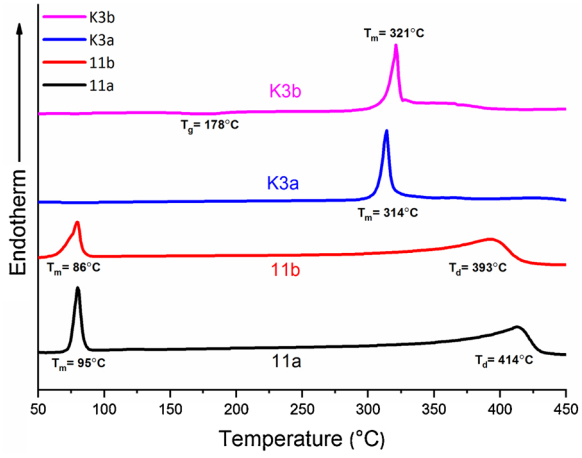

Fig. 2. DSC curves of ligands **11a** and **11b** and complexes **K3a** and **K3b**.

Table 1
Thermal properties of ligands **11a** and **11b** and complexes **K3a** and **K3b**.

Compounds	T_m (°C)	$T_d^{5\%}$ (°C)	T_g (°C)
11a	95	244	–
11b	86	233	–
K3a	314	303	–
K3b	321	313	178

complexes **K3a** and **K3b** gave both fluorescence and phosphorescence emissions (see SM, Figure S19). The observed fluorescence emission was similar to the emissions of ligand **11a** and **11b** (see SM, Figure S20). Phosphorescence emission only appeared upon de-aeration. At the highest energy excitations, it seems that intersystem crossing is not very effective between singlet states (^{1}LC/^{1}MLCT) and triplet states (^{3}LC /^{3}MLCT).

Quantum Yields: Relative fluorescent quantum yields (φ_{FL}) of ligands **11a** and **11b** were determined in dichloromethane by using Rhodamine B (φ_{FL} = 49 % in ethanol, λ_{exc} = 330 nm) as the reference [58]. Ligands **11a** and **11b** were poorly emissive, φ_{FL} of which were 0.20 % and 0.22 %, respectively. The relative phosphorescent quantum yields (φ_{PL}) of complexes **K3a** and **K3b** were determined using Ir(ppy)$_3$ (φ_{PL} = 40 % in toluene, λ_{exc} = 400 − 450 nm) as the reference [23], after degassing with nitrogen for 5 min. The φ_{PL} values of complexes **K3a** and **K3b** were 99.3 % and 79.3 %, respectively. An estimated error in quantum yield calculations is ca. 7–32 %. The details of the calculations can be found in the Supplementary Material section. Both complexes were highly emissive in comparison to Ir(pq)$_2$acac (φ_{PL} = 10 % in 2-methyltetrahydrofuran [6] or 12 % in tetrahydrofuran [32]). It is noteworthy that complex **K3a**, in which the formyl group is at the *para* position to the iridium, is significantly more emissive than complex **K3b**, in which the formyl group is at the *meta* position to the iridium. The photophysical data are summarised in Table 3.

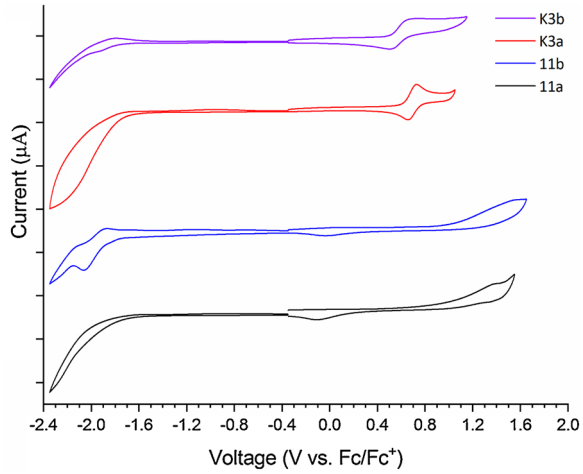

Fig. 3. Cyclic voltammograms (CV) of ligands **11a** and **11b** and complexes **K3a** and **K3b** in dichloromethane, scan rate 100 mV/s.

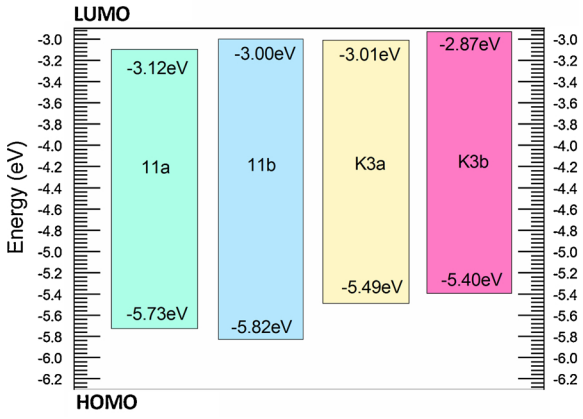

Fig. 4. Energy levels of ligands **11a** and **11b** and complexes **K3a** and **K3b**.

Electroluminescent properties: Electroluminescence (EL) properties of complexes **K3a** and **K3b** were investigated by fabricating solution-processed phosphorescent organic light emitting diodes (PhOLEDs). The device configuration was ITO/PEDOT:PSS/EML/ TPBi/ LiF/Al as depicted in Fig. 7a. In this configuration, commercial indium-doped tin oxide (ITO) was used as the anode and poly(3,4-ethylenedioxythiophene):poly(styrenesulfonate) (PEDOT:PSS) was used as a hole injection layer (HIL). The emissive layer (EML) was fabricated by mixing three different materials: poly(9-vinylcarbazole) (PVK), 2-(4-tert-butylphenyl)-5-(4-biphenylyl)-1,3,4-oxadiazole (PBD) and complex **K3a**/**K3b**. In PhOLED devices, PVK is frequently used as a host material [59], but a blend of PVK and PBD was also reported [60–64] as a mixed host system, in which PVK acts as a hole-transporting host and PBD acts as the first electron transport host. The weight percent ratio of the PVK:PBD host component was fixed as 1:0.4 according to previously reported literature [65]. This was an efficient ratio to reduce the risk of excimer formation and to increase device stability [66]. Meanwhile, we also tried to fabricate the OLED without adding PBD. Complexes **K3a** and **K3b** were used as dopant and emitter with a varying weight percentage (wt%) ratio of 5, 8 and 10. In all devices 1,3,5-tris(1-phenyl-1H-benzimidazol-2-yl)benzene) (TPBi) was used as a second electron transport layer and hole blocking layer [67,68]. Lithium fluoride (LiF)

Table 2
Reduction and oxidation potentials and energy gaps of ligands **11a** and **11b** and complexes **K3a** and **K3b**.

Compounds	E_{onset}^{red} (V)	E_{LUMO} (eV)	$E_{1/2}^{ox}$ (V)	E_{HOMO} (eV)	E_g^{elec}/E_g^{opt} (eV)
11a	−1.68	−3.12	0.93 (E_{onset})	−5.73	2.61/3.24
11b	−1.80	−3.00	1.02 (E_{onset})	−5.82	2.82/2.99
K3a	−1.79	−3.01	0.69	−5.49	2.48/2.17
K3b	−1.94	−2.87	0.60	−5.40	2.53/1.97

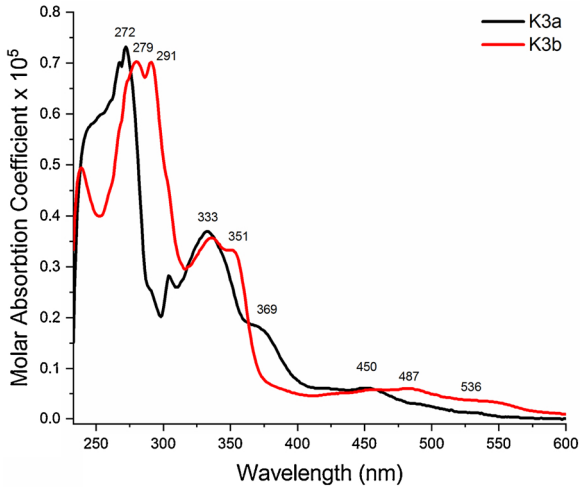

Fig. 5. UV–vis spectra of complexes **K3a** and **K3b** in dichloromethane.

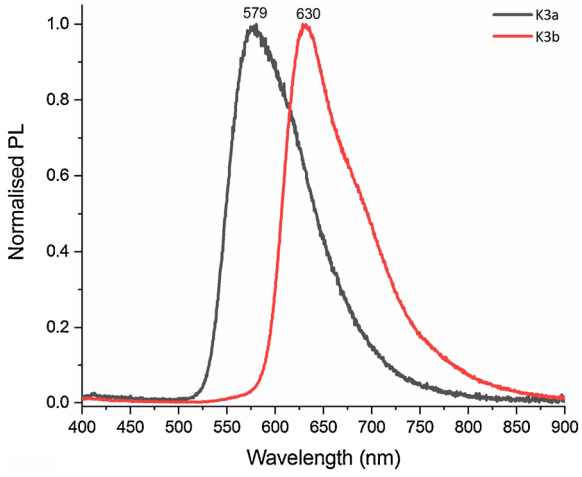

Fig. 6. PL spectra of complexes **K3a** and **K3b** in degassed dichloromethane.

Table 3
Photophysical data for ligands **11a** and **11b** and complexes **K3a** and **K3b**.

Compounds	λ_{abs} (nm) [ε, 10^5 L. mol^{-1}. cm^{-1}][a]	λ_{em} [nm][b]	φ
11a	251 [0.340], 306 [0.056], 340 [0.024]	368	0.2[d]
11b	276 [0.352], 306 [0.227], 340 [0.111]	385	0.2[d]
K3a	272 [1.201], 333 [0.597], 369 [0.291], 450 [0.092], 487 [0.049], 536 [0.019]	579[c]	99.3[e]
K3b	279 [0.897], 291 [0.922], 335 [0.456], 351 [0.413], 481 [0.082], 542 [0.041]	630[c]	73.9[e]

[a] Absorption measured in dichloromethane.
[b] Emission measured in dichloromethane.
[c] Degassed for 5 min.
[d] Measured in dichloromethane relative to Rhodamine B (φ = 0.49 in ethanol) [58] with 330 nm excitation.
[e] Measured in toluene relative to $Ir(ppy)_3$ (φ = 0.40 in toluene) [23] with 450 nm excitation. See Supplementary Material (SM) for details.

was used as the electron injection layer and Aluminum (Al) was used as the cathode.

The HOMO and LUMO energy levels and chemical structures of the materials used in the PhOLEDs are depicted in Figs. 7b-c. The HOMO and LUMO energy levels of complexes **K3a** and **K3b** were within those of the host PVK. Therefore, the complexes can harvest holes and electrons within the EML [69]. Electron injection from the cathode could have been made easier by a second electron transport layer (TPBi). However, the hole injection barrier between the anode/PEDOT:PSS and the host PVK was still high, which could cause high turn-on voltages for devices.

Current density-voltage (J–V), luminance-voltage (L–V), current efficiency-voltage and power efficiency-voltage characteristics of the PhOLEDs made with complexes **K3a** and **K3b** are plotted in Fig. 8. The lowest turn-on voltages of 4.0 V (**K3a**) and 5.0 V (**K3b**) were recorded for the PhOLEDs made with 10 wt% complexes. The highest power efficiency was recorded for device A with a value of 1.05 lm/W at 9.6 V. This power efficiency was comparable to reported literatures for red PhOLEDs [19,70,71].

A number of different OLED devices were fabricated with complexes **K3a** and **K3b** (Table 4). An OLED device made without TPBi gave no electroluminescence at all, indicating that the electron injecting barrier between the cathode (LiF/Al) and PVK was high (Fig. 7b). In devices made with TPBi, the EL spectra of complexes **K3a** and **K3b** showed three emission peaks (Fig. 9a), two of which were very low intensity whilst the other was of high intensity. Low intensity emissions at 435 nm and 450 nm were from the mixed PVK:PBD host, indicating incomplete energy transfer from host to dopant [57,59,72,73]. High intensity emissions (572 nm and 628 nm) were from the doped iridium complexes (**K3a** and **K3b**).

Complexes **K3a** and **K3b** have Commission International del'Eclairage (CIE) coordinates (x,y) of (0.51, 0.47) and (0.56, 0.34), respectively, which correspond to yellowish-orange and red emissions (Fig. 9b). The EL spectra of complexes **K3a** and **K3b** were similar to the PL spectra in dichloromethane solution with a slight blue shift of 7 nm and 2 nm, respectively, indicating that the emission originates from the same triplet states. The EL spectra remained the same under different driving voltages, indicating that EL was stable [74].

The device made from **K3a** with the composite ETL (PBD + TPBi) exhibited almost twice the luminescence (current and power efficiencies) of the single ETL (TPBi) device. It was revealed that using PBD increases device performance and decreases turn-on voltage. Also, if the ratio of complexes was increased, the luminescence values decreased due to quenching or triplet-triplet annihilation (TTA) [75]. However, the best external quantum efficiency (EQE) value was found for device A (Table 4), which was prepared with 5 wt% of **K3a**. The device performances of complexes **K3a** and **K3b** are summarised in Table 4. It is noted that devices A–D made with **K3a** had a better luminance and peak current efficiencies than devices E–G made with **K3b**. This was ascribed to the higher quantum yield of **K3a**.

A: PVK +5 wt% K3a, **B:** PVK +8 wt% K3a, **C:** PVK +8 wt% K3a +40 wt% PBD, **D:** PVK +10 wt% K3a +40 wt% PBD, **E:** PVK +5 wt% K3b, **F:** PVK +8 wt% K3b, **G:** PVK +10 wt% K3b +40 wt% PBD.

L_{max}: Maximum luminance (Brightness), CE: Peak current efficiency, EQE: Peak external quantum efficiency, PE: Power efficiency, [a]Maximum values, [b]Values at a current density of 20 mA/cm^2, CIE: Commission International del'Eclairage.

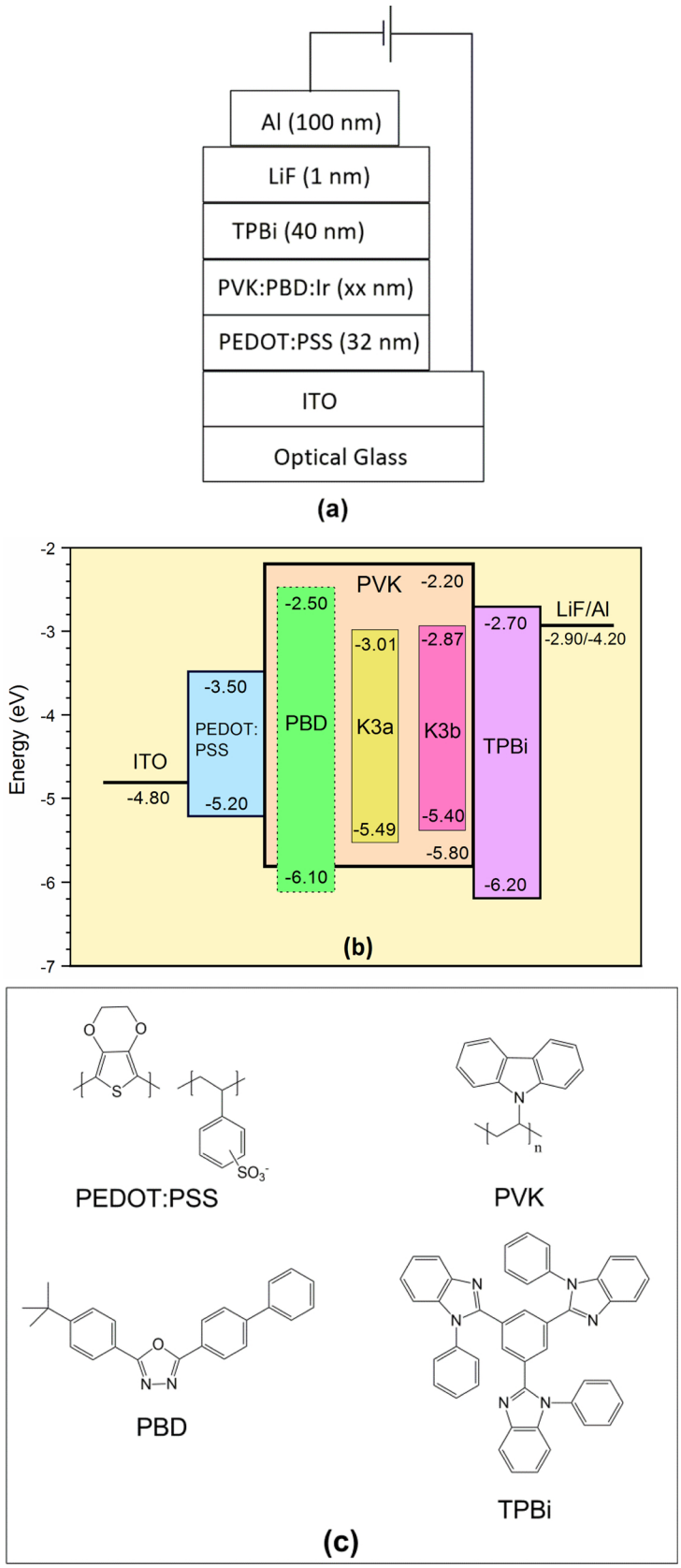

Fig. 7. (a) Device configuration in which the thickness of PVK:PBD:Ir is variable depending on the ratio, (b) HOMO-LUMO energy levels and (c) chemical structures of the materials used in electroluminescent studies.

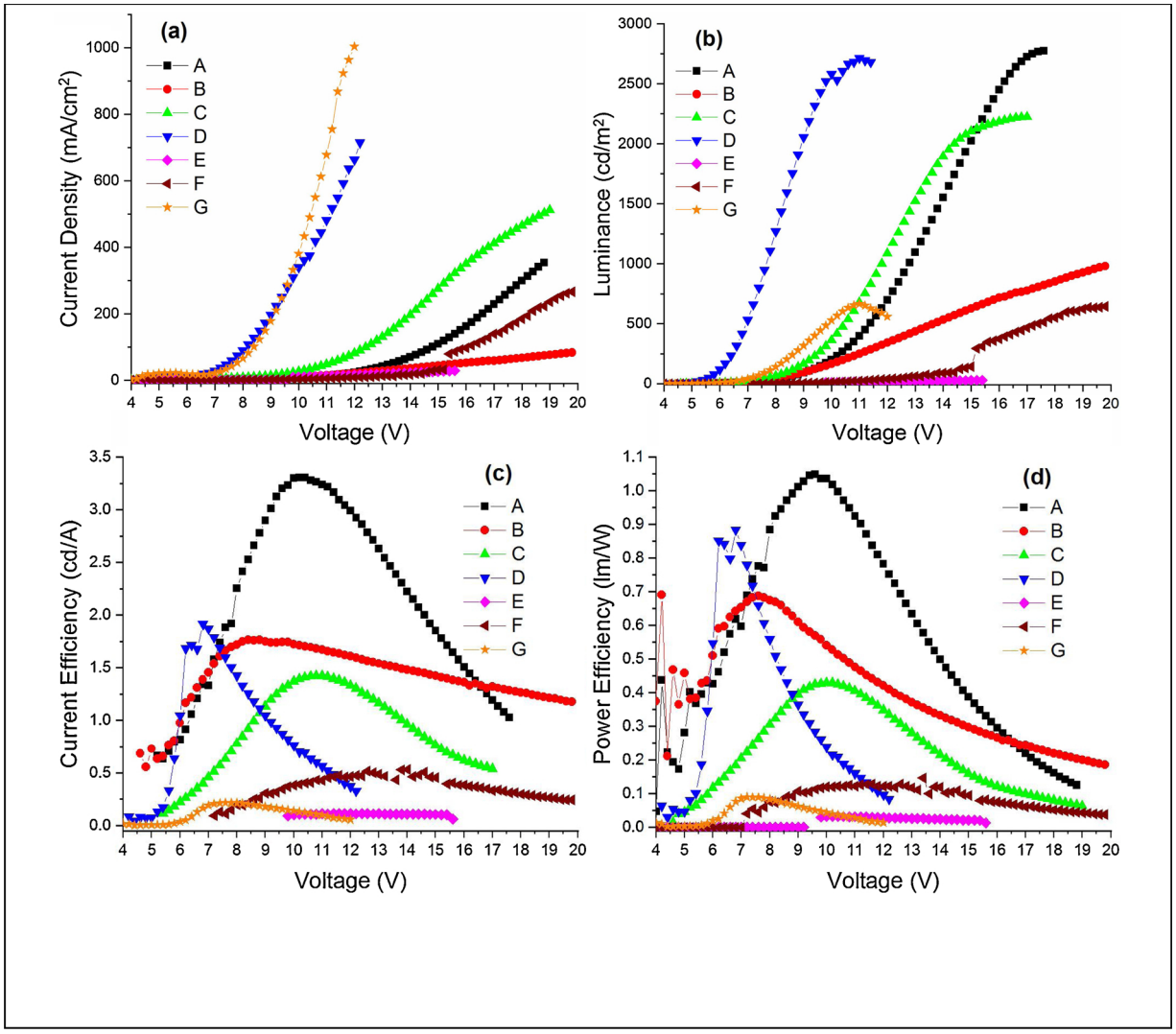

Fig. 8. (a) Current density-voltage, (b) luminance-voltage, (c) current efficiency-voltage and (d) power efficiency-voltage graphs of complexes **K3a** and **K3b**. **A:** PVK +5 wt% K3a, **B:** PVK +8 wt% K3a, **C:** PVK +8 wt% K3a +40 wt% PBD, **D:** PVK +10 wt% K3a +40 wt% PBD, **E:** PVK +5 wt% K3b, **F:** PVK +8 wt% K3b, **G:** PVK +10 wt% K3b +40 wt% PBD.

Table 4
Device (A-G) characteristics of PhOLEDs made with complexes **K3a** and **K3b**.

Device	Turn on (V)	L_{max} (cd/m^2)	CE (cd/A)	EQE (%)	PE [a/b] (lm/W)	CIE (x,y)
A	5.0	2773	3.3	1.2	1.05/0.81	0.51, 0.47
B	5.0	980	1.8	0.6	0.69/0.43	0.52, 0.47
C	4.8	2224	1.4	0.5	0.43/0.42	0.51, 0.47
D	4.0	2713	1.9	0.7	0.88/0.87	0.50, 0.46
E	–	28	0.1	0.1	0.03/0.02	0.58, 0.33
F	7.4	645	0.5	0.6	0.13/0.10	0.62, 0.33
G	5.0	665	0.2	0.2	0.09/0.08	0.56, 0.34

A: PVK +5 wt% K3a, B: PVK +8 wt% K3a, C: PVK +8 wt% K3a +40 wt% PBD, D: PVK +10 wt% K3a +40 wt% PBD, E: PVK +5 wt% K3b, F: PVK +8 wt% K3b, G: PVK +10 wt% K3b +40 wt% PBD. L_{max}: Maximum luminance (Brightness), CE: Peak current efficiency, EQE: Peak external quantum efficiency, PE: Power efficiency, [a]Maximum values, [b]Values at a current density of 20 mA/cm^2, CIE: Commission International deI'Eclairage.

4. Conclusions

In this report, two novel quinoline-based iridium(III) complexes **K3a** and **K3b** were synthesised in good yields. **K3a** and **K3b** carry a formyl group on the C-ring at the *para*- and *meta*-positions to iridium, respectively. Emission of the parent complex, Ir(pq)$_2$acac, was 20 nm blue-shifted when the formyl group was at the *para*-position to iridium (**K3a**) and was 31 nm red-shifted when the formyl group was at the *meta*-position with respect to iridium (**K3b**). Grafting a formyl group on the C-ring significantly increased the quantum yields compared to the parent complex, Ir(pq)$_2$acac, from 10 to 12% to 99 % in **K3a** and to 79 % in **K3b**.

Despite the chemical lability of the formyl group under some conditions, complexes **K3a** and **K3b** showed good thermal, electrochemical and electroluminescent stabilities. Complexes **K3a** and **K3b** were successfully used in PhOLEDs as dopants, giving EL emissions at 572 nm and 628 nm, respectively. These results clearly demonstrate the importance of structure modification for finding better dopant candidates in OLEDs.

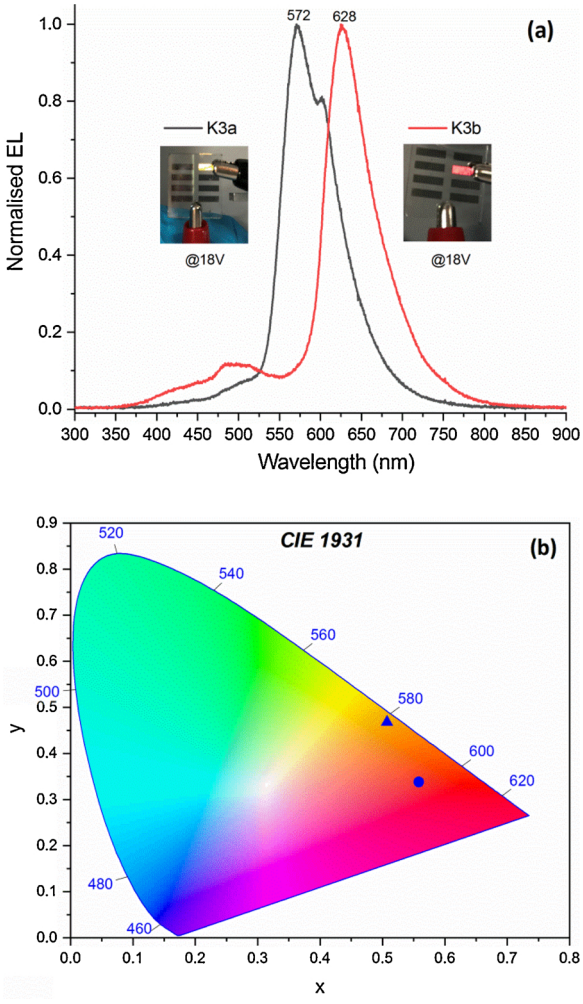

Fig. 9. (a) EL spectrum and (b) CIE coordinates (x,y) of complexes **K3a** () and **K3b** (). Insets in (a) display light coming from devices.

CRediT authorship contribution statement

Nuray Altinolcek: Investigation, Validation, Visualization. **Ahmet Battal:** Investigation, Validation, Visualization. **Mustafa Tavasli:** Conceptualization, Writing - original draft, Supervision. **Joseph Cameron:** Project administration. **William J. Peveler:** Resources, Writing - review & editing. **Holly A. Yu:** Investigation. **Peter J. Skabara:** Resources, Writing - review & editing, Supervision.

Declaration of Competing Interest

There are no conflicts to declare.

Acknowledgements

NA thanks the Scientific and Technological Research Council of Turkey (TÜBİTAK) for PhD scholarship for domestic priority areas (2211-C). AB thanks the Scientific and Technological Research Council of Turkey (TÜBİTAK) for 2219-International Postdoctoral Research Fellowship Programme for Turkish Citizens. JC and PJS thank the EPSRC for funding under grant EP/P02744X/2. WJP acknowledges the University of Glasgow for an LKAS Scholarship, and the EPSRC ECR Capital Award Scheme (EP/S017984/1) for the Duetta instrument.

Appendix A. Supplementary data

Supplementary material related to this article can be found, in the online version, at doi:https://doi.org/10.1016/j.synthmet.2020.116504.

References

[1] E. Baranoff, I. Jung, R. Scopelliti, E. Solari, M. Gratzel, M.K. Nazeeruddin, Room-temperature combinatorial screening of cyclometallated iridium(III) complexes for a step towards molecular control of colour purity, Dalton Trans. 40 (2011) 6860–6867, https://doi.org/10.1039/c0dt01697g.
[2] E. Orselli, G.S. Kottas, A.E. Konradsson, P. Coppo, R. Frohlich, L. de Cola, A. van Dijken, M. Buchel, H. Borner, Blue-emitting iridium complexes with substituted 1,2,4-triazole ligands: synthesis, photophysics, and devices, Inorg. Chem. 46 (2007) 11082–11093, https://doi.org/10.1021/ic701110p.
[3] S.I. Bezzubov, Y.M. Kiselev, A.V. Churakov, S.A. Kozyukhin, A.A. Sadovnikov, V.A. Grinberg, V.V. Emets, V.D. Doljenko, Iridium(III) 2-Phenylbenzimidazole complexes: synthesis, structure, optical properties, and applications in dye-sensitized solar cells, Eur. J. Inorg. Chem. (2016) 347–354, https://doi.org/10.1002/ejic.201501068.
[4] K. Dedeian, J. Shi, N. Shepherd, E. Forsythe, D.C. Morton, Photophysical and electrochemical properties of heteroleptic tris-cyclometalated iridium(III) complexes, Inorg. Chem. 44 (2005) 4445–4447, https://doi.org/10.1021/ic050324u.
[5] C.L. Ho, W.Y. Wong, G.H. Zhou, B. Yao, Z.Y. Xie, L.X. Wang, Solution-processible multi-component cyclometalated iridium phosphors for high-efficiency orange-emitting OLEDs and their potential use as white light sources, Adv. Funct. Mater. 17 (2007) 2925–2936, https://doi.org/10.1002/adfm.200601205.
[6] S. Lamansky, P. Djurovich, D. Murphy, F. Abdel-Razzaq, R. Kwong, I. Tsyba, M. Bortz, B. Mui, R. Bau, M.E. Thompson, Synthesis and characterization of phosphorescent cyclometalated iridium complexes, Inorg. Chem. 40 (2001) 1704–1711, https://doi.org/10.1021/ic0008969.
[7] A.B. Tamayo, B.D. Alleyne, P.I. Djurovich, S. Lamansky, I. Tsyba, N.N. Ho, R. Bau, M.E. Thompson, Synthesis and characterization of facial and meridional tris-cyclometalated iridium(III) complexes, J. Am. Chem. Soc. 125 (2003) 7377–7387, https://doi.org/10.1021/ja034537z.
[8] Z.-G. Wu, Y.-M. Jing, G.-Z. Lu, J. Zhou, Y.-X. Zheng, L. Zhou, Y. Wang, Y. Pan, Novel design of iridium phosphors with pyridinylphosphinate ligands for high-efficiency blue organic light-emitting diodes, Sci. Rep. 6 (2016) 38478, https://doi.org/10.1038/srep38478.
[9] Y. You, S.Y. Park, Phosphorescent iridium(III) complexes: toward high phosphorescence quantum efficiency through ligand control, Dalton Trans. (2009) 1267–1282, https://doi.org/10.1039/B812281D.
[10] F.J. Coughlin, M.S. Westrol, K.D. Oyler, N. Byrne, C. Kraml, E. Zysman-Colman, M.S. Lowry, S. Bernhard, Synthesis, separation, and circularly polarized luminescence studies of enantiomers of iridium(III) luminophores, Inorg. Chem. 47 (2008) 2039–2048, https://doi.org/10.1021/ic701747j.
[11] S. Ladouceur, E. Zysman-Colman, A comprehensive survey of cationic iridium(III) complexes bearing nontraditional ligand chelation motifs, Eur. J. Inorg. Chem. (2013) 2985–3007, https://doi.org/10.1002/ejic.201300171.
[12] I. Avilov, P. Minoofar, J. Cornil, L. De Cola, Influence of substituents on the energy and nature of the lowest excited states of heteroleptic phosphorescent Ir(III) complexes: a joint theoretical and experimental study, J. Am. Chem. Soc. 129 (2007) 8247–8258, https://doi.org/10.1021/ja0711011.
[13] W. Cho, G. Sarada, H. Lee, M. Song, Y.S. Gal, Y. Lee, S.H. Jin, Highly efficient, conventional and flexible deep-red phosphorescent OLEDs using ambipolar thiophene/selenophene-phenylquinoline ligand-based Ir(III) complexes, Dye. Pigment. 136 (2017) 390–397, https://doi.org/10.1016/j.dyepig.2016.08.060.
[14] Y. Jiao, M. Li, N. Wang, T. Lu, L. Zhou, Y. Huang, Z.Y. Lu, D.B. Luo, X.M. Pu, A facile color-tuning strategy for constructing a library of Ir(III) complexes with fine-tuned phosphorescence from bluish green to red using a synergetic substituent effect of -OCH3 and -CN at only the C-ring of CN ligand, J. Mater. Chem. C Mater. Opt. Electron. Devices 4 (2016) 4269–4277, https://doi.org/10.1039/c6tc00153j.
[15] M. Lepeltier, T.K.M. Lee, K.K.W. Lo, L. Toupet, H. Le Bozec, V. Guerchais, Synthesis and photophysical properties of bis-cyclometallated Iridium(III)-Styryl complexes and their saturated analogues, Eur. J. Inorg. Chem. (2007) 2734–2747, https://doi.org/10.1002/ejic.200700042.
[16] Y. You, S.Y. Park, Inter-ligand energy transfer and related emission change in the cyclometalated heteroleptic iridium complex: facile and efficient color tuning over the whole visible range by the ancillary ligand structure, J. Am. Chem. Soc. 127 (2005) 12438–12439, https://doi.org/10.1021/ja052880t.
[17] A. Kapturkiewicz, Cyclometalated iridium(III) chelates—a new exceptional class of the electrochemiluminescent luminophores, Anal. Bioanal. Chem. 408 (2016) 7013–7033, https://doi.org/10.1007/s00216-016-9615-8.
[18] T. Giridhar, W. Cho, J. Park, J.S. Park, Y.S. Gal, S. Kang, J.Y. Lee, S.H. Jin, Facile synthesis and characterization of iridium(III) complexes containing an N-ethylcarbazole-thiazole main ligand using a tandem reaction for solution processed phosphorescent organic light-emitting diodes, J. Mater. Chem. C Mater. Opt. Electron. Devices 1 (2013) 2368–2378, https://doi.org/10.1039/c3tc00323j.
[19] K.H. Lee, H.J. Kang, S.J. Lee, J.H. Seo, Y.K. Kim, S.S. Yoon, Cyclometalated iridium (III) complexes with 5-acetyl-2-phenypyridine derived ligands for red phosphorescent OLEDs, Synth. Met. 161 (2011) 1113–1121, https://doi.org/10.1016/j.synthmet.2011.03.030.

[20] C. Fan, C. Yang, Yellow/orange emissive heavy-metal complexes as phosphors in monochromatic and white organic light-emitting devices, Chem. Soc. Rev. 43 (2014) 6439–6469, https://doi.org/10.1039/c4cs00110a.
[21] C. Adachi, M.A. Baldo, S.R. Forrest, S. Lamansky, M.E. Thompson, R.C. Kwong, High-efficiency red electrophosphorescence devices, Appl. Phys. Lett. 78 (2001) 1622–1624, https://doi.org/10.1063/1.1355007.
[22] S. Lamansky, P. Djurovich, D. Murphy, F. Abdel-Razzaq, H.E. Lee, C. Adachi, P.E. Burrows, S.R. Forrest, M.E. Thompson, Highly phosphorescent bis-cyclometalated iridium complexes: synthesis, photophysical characterization, and use in organic light emitting diodes, J. Am. Chem. Soc. 123 (2001) 4304–4312, https://doi.org/10.1021/ja003693s.
[23] A. Tsuboyama, H. Iwawaki, M. Furugori, T. Mukaide, J. Kamatani, S. Igawa, T. Moriyama, S. Miura, T. Takiguchi, S. Okada, M. Hoshino, K. Ueno, Homoleptic cyclometalated iridium complexes with highly efficient red phosphorescence and application to organic light-emitting diode, J. Am. Chem. Soc. 125 (2003) 12971–12979, https://doi.org/10.1021/ja034732d.
[24] X.J. Liu, S.M. Wang, B. Yao, B.H. Zhang, C.L. Ho, W.Y. Wong, Y.X. Cheng, Z.Y. Xie, New deep-red heteroleptic iridium complex with 3-hexylthiophene for solution-processed organic light-emitting diodes emitting saturated red and high CRI white colors, Org. Electron. 21 (2015) 1–8, https://doi.org/10.1016/j.orgel.2015.02.016.
[25] J. Ding, J. Lü, Y. Cheng, Z. Xie, L. Wang, X. Jing, F. Wang, Solution-processible red iridium dendrimers based on oligocarbazole host dendrons: synthesis, properties, and their applications in organic light-emitting diodes, Adv. Funct. Mater. 18 (2008) 2754–2762, https://doi.org/10.1002/adfm.200800259.
[26] Y.-C. Chao, S.-Y. Huang, C.-Y. Chen, Y.-F. Chang, H.-F. Meng, F.-W. Yen, I.F. Lin, H.-W. Zan, S.-F. Horng, Highly efficient solution-processed red organic light-emitting diodes with long-side-chained triplet emitter, Synth. Met. 161 (2011) 148–152, https://doi.org/10.1016/j.synthmet.2010.11.013.
[27] H.U. Kim, J.H. Jang, W. Song, B.J. Jung, J.Y. Lee, D.H. Hwang, Improved luminance and external quantum efficiency of red and white organic light-emitting diodes with iridium(III) complexes with phenyl-substituted 2-phenylpyridine as a second cyclometalated ligand, J. Mater. Chem. C Mater. Opt. Electron. Devices 3 (2015) 12107–12115, https://doi.org/10.1039/c5tc02728d.
[28] T.H. Chuang, C.H. Yang, P.C. Kao, Efficient red-emitting cyclometalated iridium(III) complex and applications of organic light-emitting diode, Inorg. Chim. Acta Rev. 362 (2009) 5017–5022, https://doi.org/10.1016/j.ica.2009.08.002.
[29] L. Guang, A novel deep-red-emitting iridium complex with single-peaked narrow emission band Synthesis, photophysical properties, and electroluminescence performances, J. Lumin. 131 (2011) 184–189, https://doi.org/10.1016/j.jlumin.2010.09.032.
[30] C.L. Ho, H. Li, W.Y. Wong, Red to near-infrared organometallic phosphorescent dyes for OLED applications, J. Organomet. Chem. 751 (2014) 261–285, https://doi.org/10.1016/j.jorganchem.2013.09.035.
[31] X.W. Zhang, J. Gao, C.L. Yang, L.N. Zhu, Z.G. Li, K. Zhang, J.G. Qin, H. You, D.G. Ma, Highly efficient iridium(III) complexes with diphenylquinoline ligands for organic light-emitting diodes: synthesis and effect of fluorinated substitutes on electrochemistry, photophysics and electroluminescence, J. Organomet. Chem. 691 (2006) 4312–4319, https://doi.org/10.1016/j.jorganchem.2006.07.008.
[32] F.I. Wu, H.J. Su, C.F. Shu, L.Y. Luo, W.G. Diau, C.H. Cheng, J.P. Duan, G.H. Lee, Tuning the emission and morphology of cyclometalated iridium complexes and their applications to organic light-emitting diodes, J. Mater. Chem. 15 (2005) 1035–1042, https://doi.org/10.1039/b415754k.
[33] Y.-J. Su, H.-L. Huang, C.-L. Li, C.-H. Chien, Y.-T. Tao, P.-T. Chou, S. Datta, R.-S. Liu, Highly efficient red electrophosphorescent devices based on iridium isoquinoline complexes: remarkable external quantum efficiency over a wide range of current, Adv. Mater. 15 (2003) 884–888, https://doi.org/10.1002/adma.200304630.
[34] M.S. Park, H.J. Park, O.Y. Kim, J.Y. Lee, High color rendering index in phosphorescent white organic light-emitting diodes using a yellowish-green dopant with broad light emission, Org. Electron. 14 (2013) 1504–1509, https://doi.org/10.1016/j.orgel.2013.03.014.
[35] K.R.J. Thomas, M. Velusamy, J.T. Lin, C.-H. Chien, Y.-T. Tao, Y.S. Wen, Y.-H. Hu, P.-T. Chou, Efficient red-emitting cyclometalated iridium(III) complexes containing lepidine-based ligands, Inorg. Chem. 44 (2005) 5677–5685, https://doi.org/10.1021/ic050385s.
[36] C.A. Echeverry-Gonzalez, C.E. Puerto-Galvis, C.H. Borca, M.A. Mosquera, A.F. Luis-Robles, V.V. Kouznetsov, Optimization of the synthesis of quinoline-based neutral cyclometalated iridium complexes via microwave irradiation: design of light harvesting and emitting complexes using bulky quinolines, Org. Chem. Front. 6 (2019) 3374–3382, https://doi.org/10.1039/C9QO00870E.
[37] J.Q. Ding, J. Gao, Q. Fu, Y.X. Cheng, D.G. Ma, L.X. Wang, Highly efficient phosphorescent bis-cyclometalated iridium complexes based on quinoline ligands, Synth. Met. 155 (2005) 539–548, https://doi.org/10.1016/j.synthmet.2005.08.034.
[38] N.B. Khotele, H.K. Dahule, S.J. Dhoble, Synthesis and characterization red emitting iridium (III) complex with 2-(4-cynophenyl)-4 phenyl quinoline for PhOLEDs, Mater. Today Proc. 5 (2018) 22163–22170, https://doi.org/10.1016/j.matpr.2018.06.581.
[39] K.-H. Fang, L.-L. Wu, Y.-T. Huang, C.-H. Yang, I.W. Sun, Color tuning of iridium complexes – part I: substituted phenylisoquinoline-based iridium complexes as the triplet emitter, Inorg. Chim. Acta Rev. 359 (2006) 441–450, https://doi.org/10.1016/j.ica.2005.10.003.
[40] G.-N. Li, C.-W. Gao, H. Xie, H.-H. Chen, D. Liu, W. Sun, G.-Y. Chen, Z.-G. Niu, New luminescent cyclometalated iridium(III) complexes containing fluorinated phenylisoquinoline-based ligands: synthesis, structures, photophysical properties and DFT calculations, Chin. Chem. Lett. 27 (2016) 428–432, https://doi.org/10.1016/j.cclet.2015.12.007.
[41] N. Altinolcek, A. Battal, M. Tavasli, W.J. Peveler, H.A. Yu, P.J. Skabara, Synthesis of novel multifunctional carbazole-based molecules and their thermal, electrochemical and optical properties, Beilstein J. Org. Chem. 16 (2020) 1066–1074, https://doi.org/10.3762/bjoc.16.93.
[42] D. Wang, Y. Wu, B. Jiao, H. dong, G. Zhou, G. Wang, Z. Wu, Wide tuning of emission color of iridium (III) complexes from green to deep red via dicyanovinyl substituent effect on 2-phenylpyridine ligands, Org. Electron. 14 (2013) 2233–2242, https://doi.org/10.1016/j.orgel.2013.05.001.
[43] M.Y. Wong, G. Xie, C. Tourbillon, M. Sandroni, D.B. Cordes, A.M.Z. Slawin, I.D.W. Samuel, E. Zysman-Colman, Formylated chloro-bridged iridium(iii) dimers as OLED materials: opening up new possibilities, Dalton Trans. 44 (2015) 8419–8432, https://doi.org/10.1039/C4DT03127J.
[44] X. Qian, Y.Z. Zhu, W.Y. Chang, J. Song, B. Pan, L. Lu, H.H. Gao, J.Y. Zheng, Benzo[a]carbazole-Based donor-pi-Acceptor type organic dyes for highly efficient dye-sensitized solar cells, ACS Appl. Mater. Interfaces 7 (2015) 9015–9022, https://doi.org/10.1021/am508400a.
[45] C. Jia, N. Wu, X. Cai, G. Li, L. Zhong, L. Zou, X. Cui, Ruthenium-catalyzed meta-selective CAr—H bond formylation of arenes, J. Org. Chem. 85 (2020) 4536–4542, https://doi.org/10.1021/acs.joc.0c00007.
[46] S.-M. Li, J. Huang, G.-J. Chen, F.-S. Han, PdCl2(dppf)-catalyzed in situ coupling of 2-hydroxypyridines with aryl boronic acids mediated by PyBroP and the one-pot chemo- and regioselective construction of two distinct aryl–aryl bonds, Chem. Commun. (Camb.) 47 (2011) 12840–12842, https://doi.org/10.1039/C1CC15753A.
[47] T. Kolasa, D.E. Gunn, P. Bhatia, K.W. Woods, T. Gane, A.O. Stewart, J.B. Bouska, R.R. Harris, K.I. Hulkower, P.E. Malo, R.L. Bell, G.W. Carter, C.D.W. Brooks, Heteroarylmethoxyphenylalkoxyiminoalkylcarboxylic acids as leukotriene biosynthesis inhibitors, J. Med. Chem. 43 (2000) 690–705, https://doi.org/10.1021/jm9904102.
[48] S. Sprouse, K.A. King, P.J. Spellane, R.J. Watts, Photophysical effects of metal-carbon sigma-bonds in ortho-metalated complexes of Ir(Iii) and Rh(Iii), J. Am. Chem. Soc. 106 (1984) 6647–6653, https://doi.org/10.1021/ja00334a031.
[49] X. Li, T.N. Zang, L.S. Yu, D.Y. Zhang, G.H. Lu, H.J. Chi, G.Y. Xiao, Y. Dong, Z. Cui, Z.C. Zhang, Z.Z. Hu, A promising phosphorescent heteroleptic iridium complex with carbazole-functionalized substituent: synthesis, photophysical and electroluminescent performances, Opt. Mater. (Amst) 35 (2012) 300–306, https://doi.org/10.1016/j.optmat.2012.09.002.
[50] L.D. Bozano, K.R. Carter, V.Y. Lee, R.D. Miller, R. DiPietro, J.C. Scott, Electroluminescent devices based on cross-linked polymer blends, J. Appl. Phys. 94 (2003) 3061–3068, https://doi.org/10.1063/1.1599625.
[51] K. Scanlan, A.L. Kanibolotsky, B. Breig, G.J. Hedley, P.J. Skabara, Tetrathiafulvalene-oligofluorene star-shaped systems: new semiconductor materials for fluorescent moisture indicators, J. Mater. Chem. C Mater. Opt. Electron. Devices 7 (2019) 6582–6591, https://doi.org/10.1039/c9tc00845d.
[52] K. Zhang, Z. Chen, C.L. Yang, X.W. Zhang, Y.T. Tao, L. Duan, L. Chen, L. Zhu, J.G. Qin, Y. Cao, Improving the performance of phosphorescent polymer light-emitting diodes using morphology-stable carbazole-based iridium complexes, J. Mater. Chem. 17 (2007) 3451–3460, https://doi.org/10.1039/b705342h.
[53] S.K. Kang, J. Jeon, S.H. Jin, Y.I. Kim, Orange-yellow phosphorescent iridium(III) complex for solution-processed organic light-emitting diodes: structural, optical and electroluminescent properties of bis(2-phenylbenzothiazole)[2-(2-hydroxyphenyl) benzothiazole]iridium(III), Bull. Korean Chem. Soc. 38 (2017) 646–650, https://doi.org/10.1002/bkcs.11144.
[54] H.Z. Liu, R.C. Bo, H.F. Liu, N.J. Li, Q.F. Xu, H. Li, J.M. Lu, L.H. Wang, Study of the influences of molecular planarity and aluminum evaporation rate on the performances of electrical memory devices, J. Mater. Chem. C Mater. Opt. Electron. Devices 2 (2014) 5709–5716, https://doi.org/10.1039/c4tc00311j.
[55] S.J. Yun, H.J. Seo, M. Song, S.H. Jin, Y.I. Kim, Blue emitting cationic iridium complexes containing two substituted 2-Phenylpyridine and one 2,2' -Biimidazole for solution-processed organic light-emitting diodes (OLEDs), Bull. Korean Chem. Soc. 33 (2012) 3645–3650, https://doi.org/10.5012/bkcs.2012.33.11.3645.
[56] Y. Zhou, W. Li, L. Yu, Y. Liu, X. Wang, M. Zhou, Highly efficient electrochemiluminescence from iridium(III) complexes with 2-phenylquinoline ligand, Dalton Trans. 44 (2015) 1858–1865, https://doi.org/10.1039/c4dt02809k.
[57] B.H. Tong, Q.B. Mei, D.Y. Chen, M.G. Lu, Synthesis and electroluminescent properties of red emissive iridium(III) complexes with ester-substituted phenylquinoline ligands, Synth. Met. 162 (2012) 1701–1706, https://doi.org/10.1016/j.synthmet.2012.06.016.
[58] K.G. Casey, E.L. Quitevis, Effect of solvent polarity on nonradiative processes in xanthene dyes: rhodamine B in normal alcohols, J. Phys. Chem. 92 (1988) 6590–6594, https://doi.org/10.1021/j100334a023.
[59] H.A. Al-Attar, G.C. Griffiths, T.N. Moore, M. Tavasli, M.A. Fox, M.R. Bryce, A.P. Monkman, Highly efficient, solution-processed, single-layer, electrophosphorescent diodes and the effect of molecular dipole moment, Adv. Funct. Mater. 21 (2011) 2376–2382, https://doi.org/10.1002/adfm.201100324.
[60] J.H. Cook, H.A. Al-Attar, A.P. Monkman, Effect of PEDOT-PSS resistivity and work function on PLED performance, Org. Electron. 15 (2014) 245–250, https://doi.org/10.1016/j.orgel.2013.11.029.
[61] F.M. Hwang, H.Y. Chen, P.S. Chen, C.S. Liu, Y. Chi, C.F. Shu, F.L. Wu, P.T. Chou, S.M. Peng, G.H. Lee, Iridium(III) complexes with orthometalated quinoxaline ligands: subtle tuning of emission to the saturated red color, Inorg. Chem. 44 (2005) 1344–1353, https://doi.org/10.1021/ic0489443.
[62] S. Mulani, M. Xiao, S.J. Wang, Y.W. Chen, J.B. Peng, Y.Z. Meng, Structure properties of a highly luminescent yellow emitting material for OLED and its application, RSC Adv. 3 (2013) 215–220, https://doi.org/10.1039/c2ra21951d.
[63] R. Ragni, E.A. Plummer, K. Brunner, J.W. Hofstraat, F. Babudri, G.M. Farinola,

F. Naso, L. De Cola, Blue emitting iridium complexes: synthesis, photophysics and phosphorescent devices, J. Mater. Chem. 16 (2006) 1161–1170, https://doi.org/10.1039/b512081k.
[64] W.G. Zhang, Z.Q. He, Y.S. Wang, S.M. Zhao, Solution-processable phosphorescence based on iridium-cored small molecules with the trifluoromethyl group, Opt. Mater. (Amst) 42 (2015) 137–143, https://doi.org/10.1016/j.optmat.2014.12.033.
[65] M. Tavasli, T.N. Moore, Y.H. Zheng, M.R. Bryce, M.A. Fox, G.C. Griffiths, V. Jankus, H.A. Al-Attar, A.P. Monkman, Colour tuning from green to red by substituent effects in phosphorescent tris-cyclometalated iridium(III) complexes of carbazole-based ligands: synthetic, photophysical, computational and high efficiency OLED studies, J. Mater. Chem. 22 (2012) 6419–6428, https://doi.org/10.1039/c2jm15049b.
[66] M. Janghouri, E. Mohajerani, M.M. Amini, E. Najafi, H. Hosseini, Yellow-orange electroluminescence of novel tin complexes, J. Korean Inst. Electr. Electron. Mater. Eng. 42 (2013) 2915–2925, https://doi.org/10.1007/s11664-013-2694-9.
[67] B. Liu, M. Xu, L. Wang, H. Tao, Y. Su, D. Gao, J. Zou, L. Lan, J. Peng, Comprehensive study on the Electron transport layer in blue flourescent organic light-emitting diodes, ECS J. Solid State Sci. Technol. 2 (2013) R258–R261, https://doi.org/10.1149/2.034311jss.
[68] J.-R. Lian, F.-F. Niu, Y.-W. Liu, P.-J. Zeng, Improved hole-blocking and Electron injection using a TPBI interlayer at the cathode interface of OLEDs, Chin. Phys. Lett. 28 (2011) 047803, https://doi.org/10.1088/0256-307x/28/4/047803.
[69] F.C. Chen, S.C. Chang, G.F. He, S. Pyo, Y. Yang, M. Kurotaki, J. Kido, Energy transfer and triplet exciton confinement in polymeric electrophosphorescent devices, J. Polym. Sci.: Polym. Phys. Ed. 41 (2003) 2681–2690, https://doi.org/10.1002/polb.10648.
[70] Y. Ding, D. Liu, J. Li, H. Li, H. Ma, D. Li, R. Niu, Saturated red phosphorescent Iridium(III) complexes containing phenylquinoline ligands for efficient organic light-emitting diodes, Dye. Pigment. 179 (2020) 108405, https://doi.org/10.1016/j.dyepig.2020.108405.
[71] S.-J. Lee, J.-S. Park, M. Song, I.A. Shin, Y.-I. Kim, J.W. Lee, J.-W. Kang, Y.-S. Gal, S. Kang, J.Y. Lee, S.-H. Jung, H.-S. Kim, M.-Y. Chae, S.-H. Jin, Synthesis and characterization of red-emitting iridium(III) complexes for solution-processable phosphorescent organic light-emitting diodes, Adv. Funct. Mater. 19 (2009) 2205–2212, https://doi.org/10.1002/adfm.200900322.
[72] X. Gong, S.H. Lim, J.C. Ostrowski, D. Moses, C.J. Bardeen, G.C. Bazan, Phosphorescence from iridium complexes doped into polymer blends, J. Appl. Phys. 95 (2004) 948–953, https://doi.org/10.1063/1.1635976.
[73] Q. Zhao, C.Y. Jiang, M. Shi, F.Y. Li, T. Yi, Y. Cao, C.H. Huang, Synthesis and photophysical, electrochemical, and electrophosphorescent properties of a series of iridium(III) complexes based on quinoline derivatives and different beta-diketonate ligands, Organometallics 25 (2006) 3631–3638, https://doi.org/10.1021/om060037d.
[74] J.Y. Li, R.J. Wang, R.X. Yang, W. Zhou, X. Wang, Iridium complexes containing 2-aryl-benzothiazole ligands: color tuning and application in high-performance organic light-emitting diodes, J. Mater. Chem. C Mater. Opt. Electron. Devices 1 (2013) 4171–4179, https://doi.org/10.1039/c3tc30586d.
[75] M.J. Cho, J.I. Jin, D.H. Choi, J.H. Yoon, C.S. Hong, Y.M. Kim, Y.W. Park, B.K. Ju, Tunable emission of polymer light emitting diodes bearing green-emitting Ir(III) complexes: the structural role of 9-((6-(4-fluorophenyl)pyridin-3-yl)methyl)-9H-carbazole ligands, Dye. Pigment. 85 (2010) 143–151, https://doi.org/10.1016/j.dyepig.2009.10.017.